Available online at www.sciencedirect.com
SCIENCE DIRECT®
Biochemical and Biophysical Research Communications 330 (2005) 34–38
BBRC
www.elsevier.com/locate/ybbrc

Preserved synaptic vesicle recycling in hippocampal neurons in a mouse Alzheimer's disease model

Pamela J. Yao *, Ittai Bushlin, Katsutoshi Furukawa

Laboratory of Neurosciences, NIA/NIH, 5600 Nathan Shock Drive, Baltimore, MD 21224, USA

Received 3 February 2005

Abstract

A recently described triple-transgenic mouse model (3×Tg, $PS1_{M146V}$, APP_{Swe}, and tau_{P301L}) develops a neuropathology similar to the brains of Alzheimer's disease patients including progressive deposits of plaques and tangles [Neuron 39 (2003) 409]. These mice also show age-related deficits in hippocampal synaptic plasticity that occurs before the development of plaques and tangles. Here we report unchanged synaptic vesicle recycling, as measured by FM1-43 release, in the hippocampal neurons of the 3×Tg mice. Expression levels of presynaptic protein synaptophysin and of proteins involved in synaptic vesicle recycling including AP180, dynamin I, and synaptotagmin I also remain unaffected. These data suggest that the synaptic deficits observed in the 3×Tg neurons may not arise from the preserved synaptic vesicle recycling.
Published by Elsevier Inc.

Keywords: Alzheimer's disease; Triple-transgenic mouse model; Synapse; Synaptic vesicle recycling; FM1-43 release

Alzheimer's disease (AD) is an age-related neurodegenerative disorder. Progressive loss of cognitive function is the clinical feature of patients with AD. The characteristic pathology in the brains of AD individuals includes extracellular deposits of amyloid-β peptide (Aβ plaques) and intraneuronal neurofibrillary tangles. It is generally believed that the accumulation of plaques and tangles causes, or is largely responsible for, the neuronal degeneration in AD (for review see [2]).

In addition to the presence of plaques and tangles, brains of AD patients display alterations in synapses. Stereological and immunohistochemical analyses showed reduced numbers of synapses [3–7], and morphological analysis revealed abnormal synaptic structures [4]. AD brain tissues also exhibit reduced mRNA or protein levels of synapse-specific molecules including synaptophysin [7–9], synaptotagmin I [9–14], AP180 [12,15,16], and dynamin I [16]. Many of these changes correspond to the severity of the cognitive deficits and occur in the early stage of the disease. Thus, it is possible that functional disruption of synapses plays a role in AD.

Whereas the evidence for malfunctioning synapses in AD patients remains circumstantial, the development of animal models has enabled direct examination of the molecular basis for disrupted neuronal function. A recently described triple-transgenic mouse model (3×Tg) contains $PS1_{M146V}$, APP_{Swe}, and tau_{P301L} transgenes [1]. The 3×Tg mice display the expected plaque and tangle deposits [1,17]. Moreover, electrophysiological assessments of the hippocampal neurons from these mice show impairments in basal synaptic transmission and LTP [1]. The observation that the age-related synaptic deficits occur before the overwhelming plaque and tangle pathology supports the synaptic role in AD pathology. To assess the presynaptic function of the 3×Tg neurons, we examine synaptic vesicle recycling, as measured by FM1-43 release and by immunoblotting analysis of related proteins. We report that the hippocampal neurons of the 3×Tg mice maintain functional synaptic vesicle recycling.

* Corresponding author. Fax: +1 410 558 8323.
E-mail address: yaopa@grc.nia.nih.gov (P.J. Yao).

0006-291X/$ - see front matter. Published by Elsevier Inc.
doi:10.1016/j.bbrc.2005.02.121

Materials and methods

Animals and reagents. The derivation and characterization of the 3×Tg mice have been described in detail [1,17]. All the 3×Tg mice used in this study were 8 months old. Age-matched C57BL/6 mice were used as the non-Tg controls. All animals were handled in accordance with the NIH Guidelines for the Care and Use of Laboratory Animals.

Fluorescent styryl dye *N*-(3-triethylammoniumpropyl)-4-(4-dibutylamino styryl)pyridinium dibromide (FM1-43) was obtained from Molecular Probes (Eugene, OR). All chemicals used in synaptosomal preparation and assay were of the highest quality available.

Antibodies were purchased from the following sources: mouse monoclonal AP180 antibody AP180-I mAb (Sigma), rabbit polyclonal dynamin I antibody (Affinity Bioreagents, CO), mouse monoclonal synaptophysin antibody (SVP-38, Sigma), and rabbit polyclonal synaptotagmin I antibody (Stressgen Biotechnololgies, BC, Canada). Peroxidase-conjugated secondary antibodies were purchased from Jackson ImmunoResearch (West Grove, PA).

Preparation of synaptosomes. Synaptosomes were prepared as described [18,19]. The homogenizing solution and Percoll solutions were prepared following the exact protocol [18]. Hippocampi were dissected from 3×Tg or non-Tg control mice and immediately placed in a Teflon-glass homogenizer containing the homogenizing solution (2 mice/4 hippocampi per 2 ml solution). The tissues were gently homogenized using a tissue grinder (3431-J70, Thomas Scientific) at ~700 rpm (14 up-and-down strokes with a 30-s cooling period after first 7). The homogenate was centrifuged at ~1000*g* for 10 min. The supernatant was layered onto Percoll gradients and centrifuged at 15,000*g* for 20 min using a swinging bucket rotor (Sorvall AH-629/17). The synaptosomal fraction was collected, washed, and resuspended in a Hepes buffered solution containing (in mM): 128 NaCl, 2.4 KCl, 1.2 $MgSO_4$, 1.2 KH_2PO_4, 10 Hepes, and 10 glucose, pH 7.4. All steps were carried out at 0–4 °C.

FM1-43 uptake. Synaptosomal suspensions (1 ml from 2 hippocampi/mouse, containing ~5 μg protein) were incubated with 5 μM FM1-43 and 1 mM $CaCl_2$ for 10 min at 30 °C. Following incubation with 40 mM KCl for an additional 1 min, the synaptosomes were gently washed in the Hepes buffered solution. The synaptosomes were then re-suspended in 1 ml of the Hepes buffered solution containing 1 or 2.5 mM $CaCl_2$, or 2 mM EGTA.

Fluorescence measurements of FM1-43 release. Fluorescence measurements were carried out in a stirred cuvette using a Perkin-Elmer LS55 Luminescence Spectrometer at room temperature. The following parameters were used: excitation wavelength 488 nm (slit 4 nm), emission wavelength 565 nm (slit 8 nm), measure interval 120 s, and data collect interval 0.1 s. Each of the 1 ml synaptosomal samples was equally divided into two 0.5 ml aliquots; fluorescence of one aliquot was measured without addition of KCl, and the other aliquot was measured after addition of 80 mM KCl.

Immunoblotting. Tissue lysates from hippocampi of 3×Tg and control mice were prepared by using the same protocol as described [12]. Protein samples were divided into multiple aliquots containing the same amount of total proteins (~40 μg). One of the aliquots was evaluated by Coomassie blue-stained SDS–polyacrylamide gel for comparing protein loading among the samples (Fig. 3B); the other aliquots were used for immunoblotting analyses. Gel electrophoresis, transfer, immunoblotting, and enhanced chemiluminescent detection were performed as described [12].

Results and discussion

The styryl pyridinium dyes such as FM1-43 have proven useful for studying the dynamics of synaptic vesicles [20–22]. FM dyes preferentially and reversibly partition into the outer leaflet of the exposed membrane [20–22]. The dyes fluoresce more intensely in lipid membranes than in hydrophilic environments. When exposed to nerve terminals, FM dyes can be internalized by endocytosed synaptic vesicles, and fluorescent synaptic vesicles can be visualized once the dyes bound to the external side of the plasma membrane are washed off. When stimulated nerve terminals undergo exocytosis, synaptic vesicles will release FM dyes to the extracellular fluid and the fluorescence will decline. Thus, imaging of FM dye-stained synaptic vesicles provides information on synaptic vesicles, and thus presynaptic function of nerve terminals [20–22]. Measuring changes in FM fluorescence intensity can also be used to assess synaptic release by isolated synaptosomes [19,23].

Hippocampal synaptosomes from control wild type mice (WT) and 3×Tg mice yielded similar amount of total proteins (~5 μg protein per mouse). Equivalent amounts of synaptosomes from WT and 3×Tg mice were loaded with FM1-43. WT synaptosomes demonstrated minimal spontaneous loss of fluorescence in the absence of KCl-induced depolarization (Fig. 1A, WT—upper traces). A small rate of spontaneous decline of fluorescence in 3×Tg synaptosomal samples (e.g., Fig. 1A, 3×Tg—upper traces) was not consistently observed. In both WT and 3×Tg synaptosomes, addition of KCl (80 mM) produced an obvious and rapid drop in fluorescence (Fig. 1A, lower traces). The fluorescence loss was dependent on the presence of extracellular Ca^{2+}. While the rate of KCl-induced decline of fluorescence was similar between 1 and 2.5 mM Ca^{2+}, EGTA almost completely abolished the loss of fluorescence. This requirement for Ca^{2+} highlights the importance of Ca^{2+} in the KCl-induced synaptic release process.

Fig. 1B is a quantitative comparison of synaptosomal FM1-43 release from WT and 3×Tg mice. Consistent with the observations obtained from the fluorescence traces (Fig. 1A), synaptosomes of both mouse types showed a significant increase in FM1-43 release in response to KCl-induced depolarization and the release was Ca^{2+}-dependent. The quantitative analysis also revealed a tendency towards reduced FM1-43 release in synaptosomes from 3×Tg mice, but the difference in means did not reach statistical significance ($p = 0.401$ for 2.5 mM Ca^{2+}, $p = 0.1588$ for 1 mM Ca^{2+}).

Having compared FM1-43 release, we next examined the ability of the synaptosomes to uptake FM1-43 in WT and 3×Tg mice. Because endocytosis of synaptic vesicles is mediated through a temperature sensitive clathrin-dependent mechanism [24,25], we compared the amount of KCl-inducible FM1-43 release by the synaptosomes after loading the FM1-43 at 30 °C and at 4 °C (Fig. 2). As noted above, synaptosomes loaded at 30 °C internalized and subsequently released significant amounts of FM1-43 upon KCl depolarization. The 3×Tg synaptosomes again showed a trend, though statistically insignificant, toward a decrease in FM1-43 release

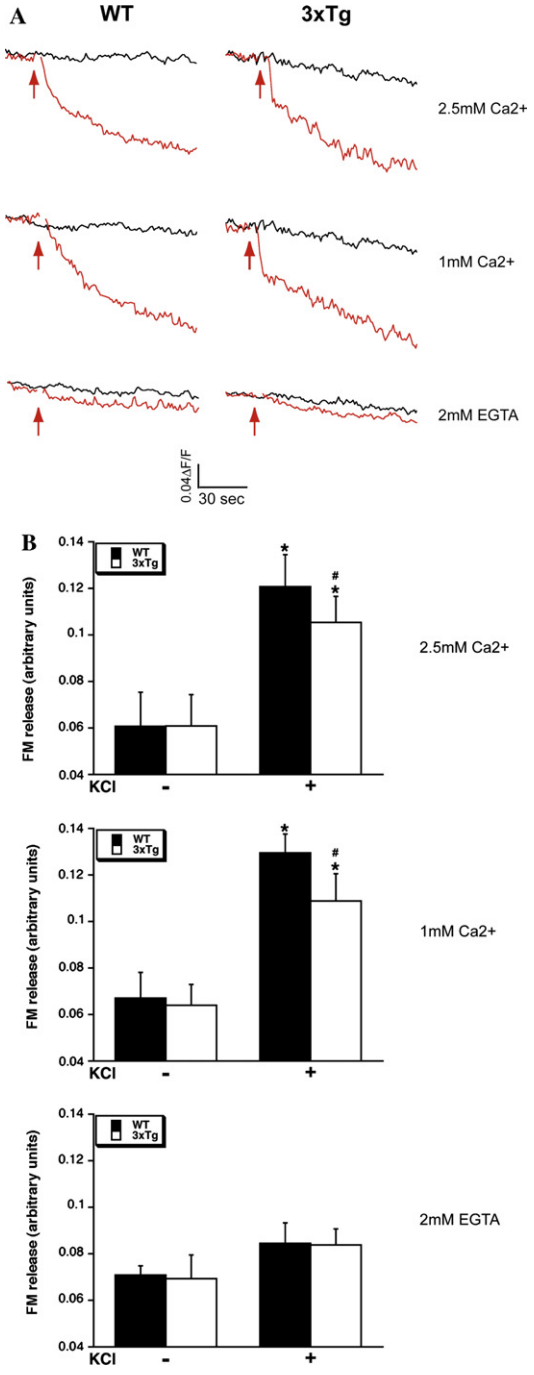

Fig. 1. Hippocampal synaptosomes from WT and 3×Tg mice exhibit similar K^+-induced, Ca^{2+}-dependent FM1-43 release. (A) Sample traces of K^+-induced decrease in fluorescence from FM1-43-loaded hippocampal synaptosomes of WT and 3×Tg mice. FM1-43 was loaded in the presence of different amounts of extracellular Ca^{2+} as indicated. Each FM1-43-loaded sample was divided into two equal aliquots. Fluorescence of one aliquot was measured without KCl-induced depolarization, and the other aliquot was used for measuring KCl-induced response. Superimposed traces from the two samples are shown. Arrows indicate the time for delivering KCl; the delivering artifacts are masked. (B) Quantitation of FM1-43 release, measured as the normalized ΔF/F (F is the average fluorescence of the initial 10 s; ΔF is the average fluorescence of the last 10 s subtract the initial fluorescence). Histograms show mean ± SEM ($n = 4$–12). $^*p < 0.01$ compared with non-K^+-induced FM release; $^{\#}p > 0.05$ compared with WT.

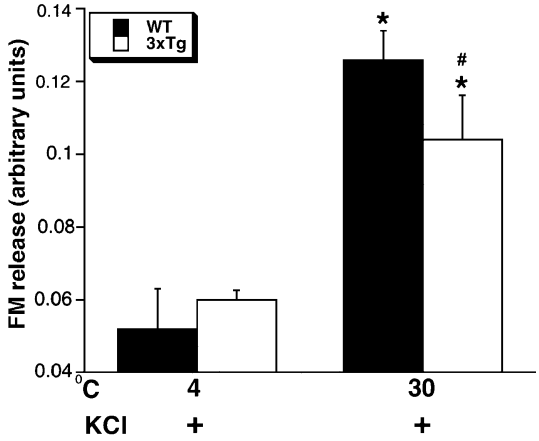

Fig. 2. Uptake of FM1-43 by hippocampal synaptosomes of WT and 3×Tg is temperature dependent. Each synaptosomal sample from WT or 3×Tg hippocampus was divided into two equal aliquots. One aliquot was loaded with FM1-43 at 30 °C; the other aliquot was loaded at 4 °C. K^+-induced FM1-43 release from the samples was then measured and quantified as the normalized ΔF/F. Histograms show mean ± SEM ($n = 3$). $^*p < 0.01$ compared with 4 °C; $^{\#}p > 0.05$ compared with WT.

($p = 0.237$). When loaded at 4 °C, synaptosomes produced almost no KCl-induced FM1-43 release, and this was true for both WT and 3×Tg (Fig. 2).

The KCl-induced, Ca^{2+}-dependent FM1-43 release and the temperature-dependent FM1-43 uptake validate the assay and confirm the functional integrity of the synaptosomal preparation. The 3×Tg synaptosomes did not display a statistically significant change in FM1-43 release, suggesting that the synaptic vesicle endo/exocytosis part of presynaptic function is normal in the 3×Tg neurons. Our data are consistent with the observation by Oddo et al. [1], in which the hippocampal slices of 3×Tg mice showed normal paired-pulse facilitation, an indirect assessment for presynaptic release mechanism. We also examined the expression levels of AP180, dynamin, synaptotagmin I, and synaptophysin. AP180, dynamin I, and synaptotagmin I are well characterized for their roles in specific steps of synaptic vesicles trafficking (for review see [26] and references within), whereas synaptophysin is a commonly used presynaptic marker [7–9]. As shown in Fig. 3, the gross levels of these proteins from 3×Tg hippocampus were not different from the WT mice.

One potential explanation for the observation of the unchanged presynaptic function in the 3×Tg neurons is that the synaptic impairments in AD primarily stem from defects in postsynaptic components or pathways. Presynaptic function, at least assessed by electrophysiologic study [1] and FM1-43 analysis (this study), may remain normal, or reasonably functional, until much later into the course of the disease. This explanation, however, does not support the findings in postmortem human studies. The AD brain tissues contain significantly reduced mRNA or protein levels of molecules with specific presyn-

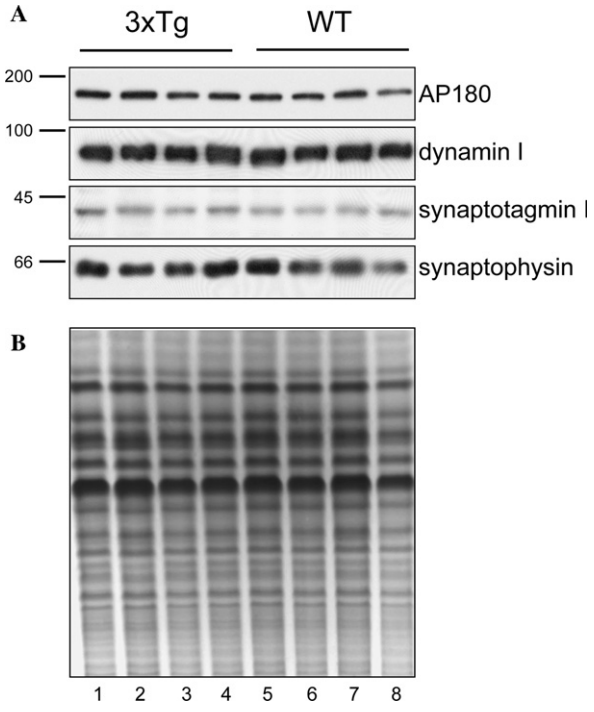

Fig. 3. Immunoblot analysis of hippocampal tissues of 3×Tg and WT mice. (A) Aliquots of lysates containing approximately same amount proteins from 3×Tg (lanes 1–4) and WT mice (lanes 5–8) were analyzed by immunoblotting using antibodies indicated. (B) Coomassie blue-stained gel showing approximately equal protein loading among the samples.

aptic functions [7–16]; and available data thus far do not suggest similar changes for postsynaptic molecules [16]. An alternative explanation for these results of 3×Tg mice is the differences between the mouse model and the human disease. Although the neuropathology of 3×Tg mice appears similar to what is consistently found in AD, the synaptic changes at the molecular level may not completely recapitulate the pathology in humans. The specific effects of mutations of APP, presenilin-1, and tau (thus 3×Tg) may not be sufficient to produce the exact neuronal phenotype attributed to AD.

Acknowledgments

We thank Dr. Mollie K. Meffert on advice for synaptosomal FM1-43 uptake assay in the early course of this work; Dr. Raphael DeCabo for allowing the use of the luminescence spectrometer; and Drs. Stuart Maudsley, Sic L. Chan, and Mark P. Mattson for helpful comments on the manuscript.

References

[1] S. Oddo, A. Caccamo, J.D. Shepherd, M.P. Murphy, T.E. Golde, R. Kayed, R. Metherate, M.P. Mattson, Y. Akbari, F.M. LaFerla, Triple-transgenic model of Alzheimer's disease with plaques and tangles: intracellular Aβ and synaptic dysfunction, Neuron 39 (2003) 409–421.
[2] M.P. Mattson, Pathways towards and away from Alzheimer's disease, Nature 430 (2004) 631–639.
[3] S.T. DeKosky, S.W. Scheff, Synapse loss in frontal cortex biopsies in Alzheimer's disease: correlation with cognitive severity, Ann. Neurol. 27 (1990) 457–464.
[4] S.W. Scheff, S.T. DeKosky, D.A. Price, Quantitative assessment of cortical synaptic density in Alzheimer's disease, Neurobiol. Aging 11 (1990) 29–37.
[5] R.D. Terry, E. Masliah, D.P. Salmon, N. Butters, R. DeTeresa, R. Hill, L.A. Hansen, R. Katzman, Physical basis of cognitive alterations in Alzheimer's disease: synapse loss is the major correlate of cognitive impairment, Ann. Neurol. 30 (1991) 572–580.
[6] M.J. West, P.D. Coleman, D.G. Flood, J.C. Troncoso, Differences in the pattern of hippocampal neuronal loss in normal ageing and Alzheimer's disease, Lancet 344 (1994) 769–772.
[7] E. Masliah, M. Mallory, M. Alford, R. DeTeresa, L.A. Hansen, D.W. McKell, J.C. Morris, Altered expression of synaptic proteins occurs early during progression of Alzheimer's disease, Neurology 56 (2001) 127–129.
[8] O. Heinonen, H. Soininen, H. Sorvari, O. Kosunen, L. Paljarvi, E. Koivisto, P.J. Riekkinen, Loss of synaptophysin-like immunoreactivity in the hippocampal formation is an early phenomenon in Alzheimer's disease, Neuroscience 64 (1995) 375–384.
[9] C.I. Sze, H. Bi, B.K. Kleinschmidt-DeMasters, C.M. Filley, L.J. Martin, Selective regional loss of exocytotic presynaptic vesicle proteins in Alzheimer's disease brains, J. Neurol. Sci. 175 (2000) 81–90.
[10] B.C. Yoo, N. Cairns, M. Fountoulakis, G. Lubec, Synaptosomal proteins, beta-soluble N-ethylmaleimide-sensitive factor attachment protein (beta-SNAP), gamma-SNAP and synaptotagmin I in brain of patients with Down syndrome and Alzheimer's disease, Dement. Geriatr. Cogn. Disord. 12 (2001) 219–225.
[11] E.J. Mufson, S.E. Counts, S.D. Ginsberg, Gene expression profiles of cholinergic nucleus basalis neurons in Alzheimer's disease, Neurochem. Res. 27 (2002) 1035–1048.
[12] P.J. Yao, P.D. Coleman, Reduction of O-linked N-acetylglucosamine-modified assembly protein-3 in Alzheimer's disease, J. Neurosci. 18 (1998) 2399–2411.
[13] S.D. Ginsberg, S.E. Hemby, V.M. Lee, J.H. Eberwine, J.Q. Trojanowski, Expression profile of transcripts in Alzheimer's disease tangle-bearing CA1 neurons, Ann. Neurol. 48 (2000) 77–87.
[14] J.F. Loring, X. Wen, J.M. Lee, J. Seilhamer, R. Somogyi, A gene expression profile of Alzheimer's disease, DNA Cell Biol. 20 (2001) 683–695.
[15] P.J. Yao, R. Morsch, L.M. Callahan, P.D. Coleman, Changes in synaptic expression of clathrin assembly protein AP180 in Alzheimer's disease analysed by immunohistochemistry, Neuroscience 94 (1999) 389–394.
[16] P.J. Yao, M. Zhu, E.I. Pyun, A.I. Brooks, S. Therianos, V.E. Meyers, P.D. Coleman, Defects in expression of genes related to synaptic vesicle trafficking in frontal cortex of Alzheimer's disease, Neurobiol. Dis. 12 (2003) 97–105.
[17] S. Oddo, A. Caccamo, M. Kitazawa, B.P. Tseng, F.M. LaFerla, Amyloid deposition precedes tangle formation in a triple transgenic model of Alzheimer's disease, Neurobiol. Aging 24 (2003) 1063–1070.
[18] A. Nagy, A.V. Delgado-Escueta, Rapid preparation of synaptosomes from mammalian brain using nontoxic isoosmotic gradient material (Percoll), J. Neurochem. 43 (1984) 1114–1123.
[19] M.K. Meffert, B.A. Premack, H. Schulman, Nitric oxide stimulates Ca(2+)-independent synaptic vesicle release, Neuron 12 (1994) 1235–1244.
[20] W.J. Betz, G.S. Bewick, Optical analysis of synaptic vesicle recycling at the frog neuromuscular junction, Science 255 (1992) 200–203.

[21] T.A. Ryan, H. Reuter, B. Wendland, F.E. Schweizer, R.W. Tsien, S.J. Smith, The kinetics of synaptic vesicle recycling measured at single presynaptic boutons, Neuron 11 (1993) 713–724.
[22] A.R. Kay, A. Alfonso, S. Alford, H.T. Cline, A.M. Holgado, B. Sakmann, V.A. Snitsarev, T.P. Stricker, M. Takahashi, L.G. Wu, Imaging synaptic activity in intact brain and slices with FM1-43 in *C. elegans*, lamprey, and rat, Neuron 24 (1999) 809–817.
[23] B. Marks, H.T. McMahon, Calcium triggers calcineurin-dependent synaptic vesicle recycling in mammalian nerve terminals, Curr. Biol. 8 (1998) 740–749.
[24] P. DeCamili, V. Slepnev, O. Shupliakov, L. Brodin, Synaptic vesicle endocytosis, in: T.C. Sudhof, C.F. Stevens (Eds.), Synapses, The Johns Hopkins University Press, Baltimore, MD, 2000, pp. 217–274.
[25] J.R. Morgan, G.J. Augustine, E.M. Lafer, Synaptic vesicle endocytosis: the races, places, and molecular faces, NeuroMolecular Med. 2 (2002) 101–114.
[26] P.J. Yao, Synaptic frailty and clathrin-mediated synaptic vesicle trafficking in Alzheimer's disease, Trends Neurosci. 27 (2004) 24–29.